ChemComm

COMMUNICATION

View Article Online
View Journal | View Issue

Cite this: *Chem. Commun.*, 2025, **61**, 11637

Received 28th February 2025,
Accepted 23rd June 2025

DOI: 10.1039/d5cc01112d

rsc.li/chemcomm

Organometallic and zeolitic ultralight MOFs from lithium alkynyl building blocks†

Ruichen Zhang,[a] Tom O'Brien,[a] Fauzi Abdilah,[ab] Andrew J. P. White,[a] Paul D. Lickiss[a] and Robert P. Davies*[a]

Organometallic lithium–carbon(alkynyl) secondary building units have been used to construct a range of novel one-, two-, and three-dimensional lithium metal organic framework (MOF) materials. The 3D Li-MOF exhibits a zeolitic lta topology, and is notable for its low density and high theoretical porosity.

Over the past two decades, the field of metal–organic frameworks (MOFs) and related reticular structures has experienced significant growth with the MOF subset in the CSDS database now comprising of over 120 000 structures (Database CSD version 5.44 Jun 2023).[1] The majority of these MOFs are constructed from transition metal centers or nodes combined with organic linkers based on carboxylic acids or nitrogen-containing heterocycles. However, a smaller subset of lithium-based MOFs has been explored as 'ultralight' materials for portable applications, such as hydrogen or methane storage, where weight is often a critical factor.[2,3] These lithium MOFs have often employed carboxylic acid or nitrogen-based heterocycle linkers repurposed from transition metal MOF studies, and as a result commonly contain extended (1D, 2D or even 3D) rather than discrete (0D) metal-based nodes.[4,5] This can lead to minimal or no porosity in the resultant materials. By leveraging alternative functionalities and adapting well-known lithium stacking and laddering principles,[6] we aim to generate discrete lithium secondary building units (Li SBUs) that can be assembled into innovative ultralight porous MOF materials.

In the work reported herein the use of organometallic lithium acetylide based clusters for MOF construction is explored. In addition to offering a potential new pathway to ultralight MOF materials, this research aims to enhance our understanding of aggregation modes for lithium acetylides which are less studied compared to those for lithium amides, imides, and aryl/alk-oxides.[6] Moreover, the use of metal – carbon bonds for MOF construction remains largely unexplored, with the first examples of metal acetylide MOFs only recently reported for copper(I)[7] and silver(I)[8] materials.

Initial efforts focussed upon building lithium acetylide secondary building units (SBUs) and then connecting these together to form coordination networks using 1,4-dioxane as a bridging ligand. Using this approach, the oxygen atoms in the dioxane can act as Lewis base donors to diametrically opposed lithium cations, thus acting as linkers for adjacent SBUs. A similar approach has previously been shown to be successful by Henderson and colleagues for the assembly of $Li_4(OAr)_4$ cubane clusters into networks.[9,10]

Three acetylenes – phenylacetylene, trimethylsilylacetylene, and cyclopropylacetylene – were initially examined. Metallation of the acetylene with *n*BuLi in a mixed hexane–dioxane solvent followed by recrystallisation led to the formation of three corresponding coordination network/MOF structures (**IMP-35**, **IMP-36** and **IMP-37**) which have been characterised using single crystal X-ray diffraction (see ESI† for full details). Each new Li-MOF contains a unique lithium acetylide SBU determined in part by the steric and electronic requirements of the original acetylene.

$[Li_2(C{\equiv}CPh)_2(dioxane)_2]$ (**IMP-35**) contains dimeric SBUs based upon four-membered Li_2C_2 rings (Fig. 1a). The carbanion centres on the acetylide asymmetrically bridge two lithium cations. A similar dimeric motif has been previously reported for $[LiC{\equiv}CPh(tmpda)]_2$ where tmpda is the bidentate ligand *N,N,N′,N′*-tetramethyl-1,3-propanediamine.[11] Each lithium in **IMP-35** coordinates to two oxygen atoms from two different dioxane molecules. These dioxanes sit almost perpendicular to the Li_2C_2 rings and form double bridges to adjacent SBUs to give a 1D polymeric motif (Fig. 1b). These 1D chains are aligned along the crystallographic 100 direction with voids between the chains containing additional non-coordinated dioxane molecules (one per SBU, see ESI†).

[a] *Department of Chemistry, Molecular Sciences Research Hub, Imperial College White City Campus, Wood Lane, London W12 0BZ, UK. E-mail: r.davies@imperial.ac.uk*
[b] *Department of Chemical Engineering, Politeknik Negeri Bandung, Bandung 40559, Indonesia*

† Electronic supplementary information (ESI) available: Full experimental and crystallographic details. CCDC 2383649–2383652. For ESI and crystallographic data in CIF or other electronic format see DOI: https://doi.org/10.1039/d5cc01112d

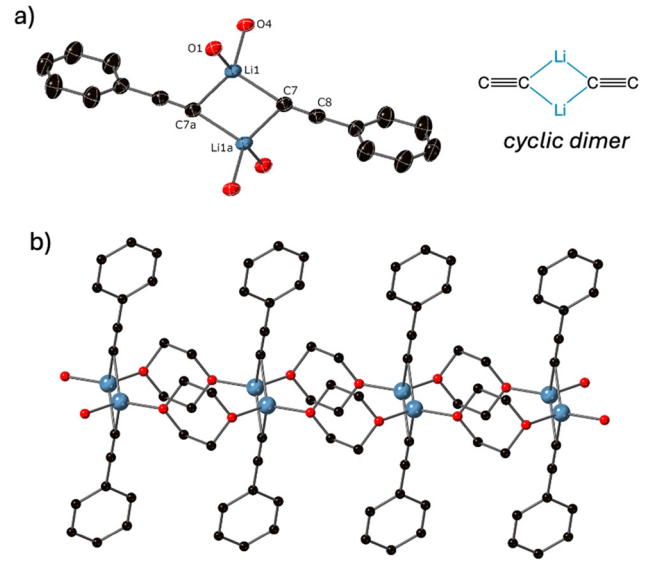

Fig. 1 (a) Molecular structure of the SBU in **IMP-35** and a simplified schematic of its core. Thermal ellipsoids shown at 40% probability. (b) View of a section of the extended 1D structure in **IMP-35**. C: black, O: red, Li: grey blue, H atoms are omitted for clarity.

In contrast $[Li_4(C{\equiv}CSiMe_3)_4(dioxane)_3]$ (**IMP-36**) is built from tetrametallic SBUs based upon a four-rung ladder structural motif (Fig. 2a). Although aggregation *via* laddering is well known for lithium amides ($LiNR_2$),[6] as far as we are aware this is the first example of laddering in lithium acetylide chemistry. Each lithium is four coordinate, with the outer lithium cations (Li1 and Li4) coordinated by two acetylide and two dioxane molecules and the inner lithium cations (Li2 and Li3) by three acetylides and one dioxane. The six dioxane molecules form linkages to four adjacent SBUs *via* two double bridges (similar to those observed in **IMP-35**) and two single bridges. This results in the formation of a 2D square grid material (Fig. 2b) with Li_4C_4 SBU nodes and **sql** topology.[12] Additional non-coordinated dioxane molecules are sited in the pores (one per SBU, see ESI†).

Use of the less sterically bulky cyclopropylacetylene gave the novel structure $[Li_8(C{\equiv}CC_3H_4)_8(dioxane)_4]$ (**IMP-37**). In this material two Li_4C_4 hetero-cubanes are joined together along one edge to form an octametallic Li_8C_8 SBU (Fig. 3a). Cubane formation for lithium acetylides has been previously reported in the literature, for example in the structures of $[(LiC{\equiv}CPh)_4(tmhda)_2]$[13] and $[(LiC{\equiv}CtBu)_4(thf)_4]$.[14] In addition, the fusion of several cubanes to form extended aggregates has also been documented for the decamer $[(LiC{\equiv}CtBu)_{10}(Et_2O)_4]$[15] and dodecamer $[(LiC{\equiv}CtBu)_{12}(thf)_4]$.[14] However, in these previously reported structures the hetero-cubanes are face sharing (also referred to as stacking of cyclic Li_2C_2 units[16]), rather than the novel edge sharing motif seen in **IMP-37**. Each lithium cation in **IMP-37** is four coordinate, with six of the eight lithium cations (those in the non-edge sharing positions – Li1, Li2 and Li3) also coordinating to the oxygen centre of a dioxane molecule. Four of these six dioxanes then bridge to neighbouring Li SBUs, whilst the other two dioxanes are mono-coordinate and hence topologically redundant. This gives an overall 2D layered network structure for **IMP-37** (Fig. 3b). Considering each Li SBU as a separate four-connecting topological point allows assignment as **sql** topology.[12]

Encouraged by these initial attempts, we then sought to incorporate the Lewis donor site into the acetylide unit itself, thus negating the need for additional dioxane molecules to

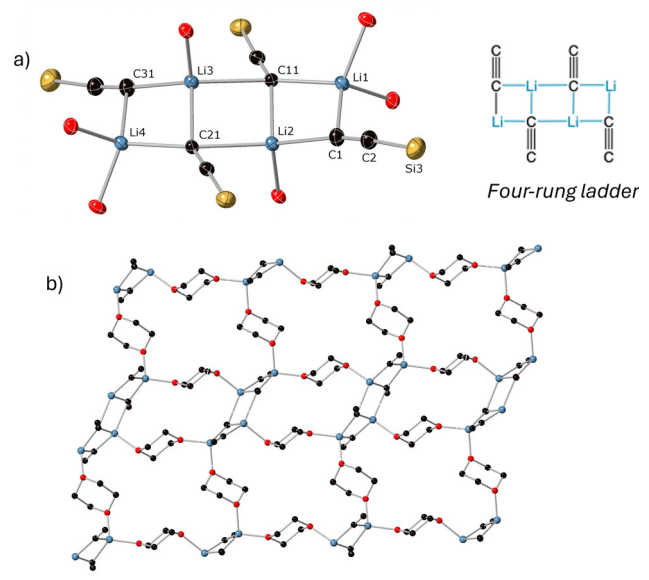

Fig. 2 (a) Molecular structure of the SBU in **IMP-36** and a simplified schematic of its core. Thermal ellipsoids shown at 40% probability. (b) View of a section of the extended 2D sheets in **IMP-36**. C: black, O: red, Li: grey blue, Si: gold, H atoms are omitted for clarity.

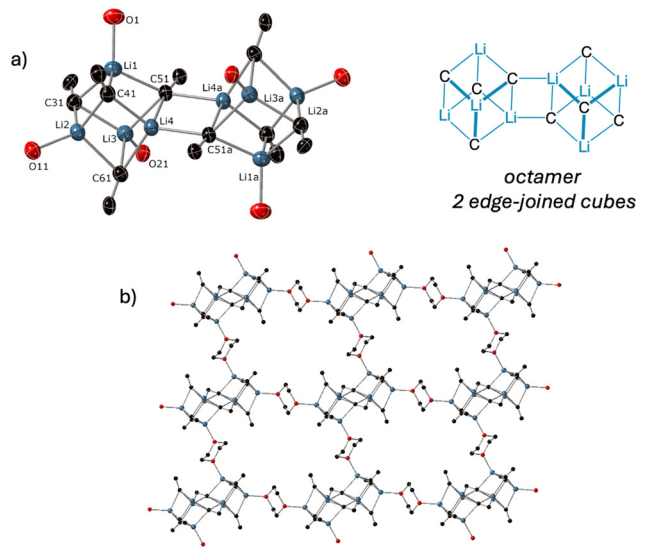

Fig. 3 (a) Molecular structure of the SBU in **IMP-37** and a simplified schematic of its core. Thermal ellipsoids shown at 30% probability. (b) View of a section of the extended 2D sheets in **IMP-37** with cyclopropyl groups and non-bridging dioxanes omitted for clarity. C: black, O: red, Li: grey blue, H atoms are omitted for clarity.

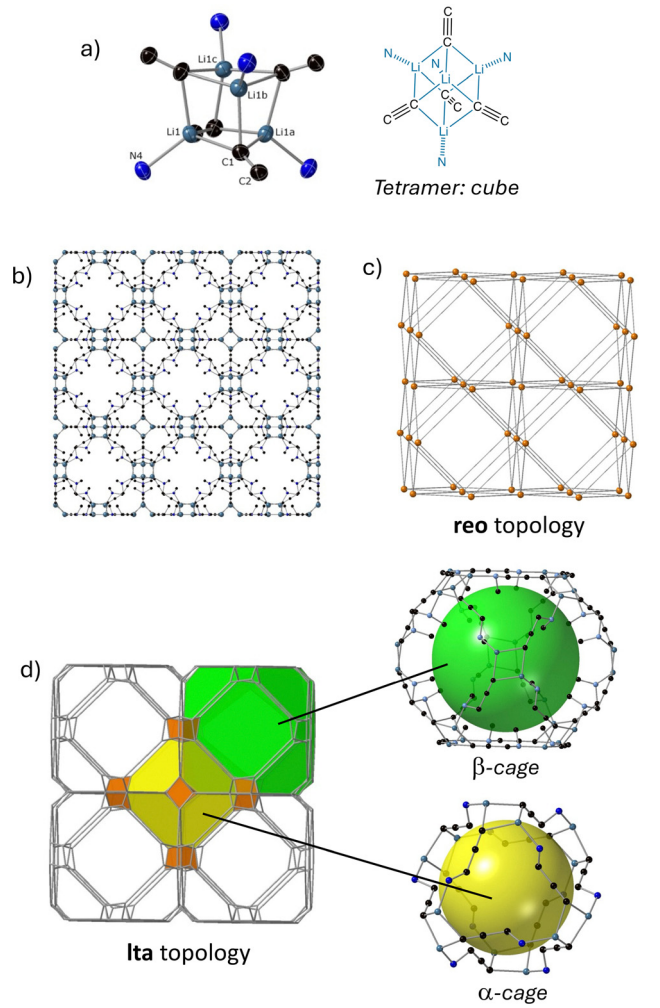

Fig. 4 (a) Molecular structure of the SBU in **IMP-38** and a simplified schematic of its core. Thermal ellipsoids shown at 30% probability; (b) view of a section of the extended 3D structure in **IMP-38** with cyclopropyl groups and non-bridging dioxanes omitted for clarity. (c) Topological map assuming unimodal 8-c nodes based on Li_4C_4 cubanes; (d) topological map for **IMP-28** in which individual metal and carbonanion centres act as 4-c nodes. C: black, N: blue, Li: grey blue, H atoms are omitted for clarity.

connect the SBUs. Hence, metalation of 3-dimethylamino-1-propyne containing a Lewis Basic amine functionality led to the new 3D-periodic structure $[Li_4(C{\equiv}CCH_2NMe_2)_4]$ **IMP-38**. Interestingly this MOF material could be obtained from a range of different solvent systems, including in the presence of coordinating solvents such as dioxane without any dioxane incorporation into the 3D network.

Initial inspection of **IMP-38** reveals the presence of Li_4C_4 cubane SBUs (Fig. 4a). As well as bridging three acetylide carbanions, each lithium cation in the SBU is also coordinated by the nitrogen atom of an adjacent dimethylaminopropynide unit. This results in the assembly of the cubic 8-connected SBUs into a 3D-periodic structure (Fig. 4b) with **reo** topology and point symbol $(3^8{\cdot}4^8{\cdot}5^8{\cdot}6^4)$ (Fig. 4c). However, a more holistic view of **IMP-38** in which the individual lithium and carbanion centres are considered as individual topological nodes, reveals a **lta** topology (Fig. 4d), which although well known in zeolite chemistry is currently rare for MOF materials. This topology is based upon Linde Type A zeolite where Li cations in **IMP-38** are surrogate for the Al cations in the zeolite, acetylide carbanions for Si, and the bent CCH_2NMe_2 unit (C–C–N bond angle 114.6°) a direct replacement for the di-coordinate oxygen. The α and β (sodalite) zeolite cages can be clearly identified within the MOF (Fig. 4d) with approximate diameters of 13.0 and 11.6 Å respectively (shortest atom to atom distance).

IMP-38 is amongst the most porous of all Li-MOFs reported to date with a calculated void volume of 29.1%,[17] a calculated gravimetric surface area of 534 $m^2\ g^{-1}$ (volumetric surface area = 431 $m^2\ cm^{-3}$)[18] and a density of 0.806 $g\ cm^{-3}$ assuming removal of all non-coordinated solvents from within the pores. The maximum pore diameter is 8.62 Å with a pore limiting diameter of 2.53 Å,[18] suggesting it is well suited for potential applications in dihydrogen storage, but less so for larger molecules such as CO_2. However, despite these promising theoretical porosity values, it has not been possible to verify them experimentally since **IMP-38** undergoes rapid decomposition in air/moisture leading to the formation of LiOH as shown using powder diffraction studies (see Fig. S2.5, ESI†). Despite this we believe this work presents a significant advance in the field of MOF chemistry, being the first example of a new class of zeolitic ultralight Li-MOF material. Studies to extrapolate this work to other metals and linkers using a reticular approach are currently underway, with a goal to improve the stability and porosity of the resultant MOFs to enable practical applications.

We thank Indonesia Endowment Fund For Education (LPDP) for funding (PhD Scholarship to F.A.).

Conflicts of interest

There are no conflicts to declare.

Data availability

Experimental data supporting this article have been included as part of the ESI.† Crystallographic data for **IMP-35**, **IMP-36**, **IMP-37** and **IMP-38** has been deposited at the Cambridge Crystallographic data centre (CCDC) under numbers 2383649 to 2383652, respectively. Additional information on the data refinements is included in the ESI.†

References

1 P. Z. Moghadam, A. Li, S. B. Wiggin, A. Tao, A. G. P. Maloney, P. A. Wood, S. C. Ward and D. Fairen-Jimenez, *Chem. Mater.*, 2017, **29**, 2618–2625.
2 M. A. Alnaqbi, A. Alzamly, S. H. Ahmed, M. Bakiro, J. Kegere and H. L. Nguyen, *J. Mater. Chem. A*, 2021, **9**, 3828–3854.
3 D. Banerjee and J. B. Parise, *Cryst. Growth Des.*, 2011, **11**, 4704–4720.
4 D. Pugh, E. Ashworth, K. Robertson, L. C. Delmas, A. J. P. White, P. N. Horton, G. J. Tizzard, S. J. Coles, P. D. Lickiss and R. P. Davies, *Cryst. Growth Des.*, 2018, **19**, 487–497.
5 B. F. Abrahams, M. J. Grannas, T. A. Hudson and R. Robson, *Angew. Chem., Int. Ed.*, 2010, **49**, 1087–1089.
6 R. E. Mulvey, *Chem. Soc. Rev.*, 1991, **20**, 167–209.

7 L. Jiang, J. Jia, Y. Ma, Y. Tian, X. Zou and G. Zhu, *Chem*, 2024, **10**, 557–566.
8 L. Jiang, L. Lin, Z. Wang, H. Ai, J. Jia and G. Zhu, *J. Am. Chem. Soc.*, 2024, **146**, 22930–22936.
9 D. J. MacDougall, J. J. Morris, B. C. Noll and K. W. Henderson, *Chem. Commun.*, 2005, 456–458.
10 J. J. Morris, D. J. Macdougall, B. C. Noll and K. W. Henderson, *Dalton Trans.*, 2008, 3429–3437.
11 B. Schubert and E. Weiss, *Chem. Ber.*, 2006, **116**, 3212–3215.
12 M. O'Keeffe, M. A. Peskov, S. J. Ramsden and O. M. Yaghi, *Acc. Chem. Res.*, 2008, **41**, 1782–1789.
13 B. Schubert and E. Weiss, *Angew. Chem., Int. Ed.*, 2003, **22**, 496–497.
14 M. Geissler, J. Kopf, B. Schubert, E. Weiss, W. Neugebauer and P. V. R. Schleyer, *Angew. Chem., Int. Ed.*, 2003, **26**, 587–588.
15 A. M. Borys and E. Hevia, *Chem. Commun.*, 2023, **59**, 7032–7035.
16 D. R. Armstrong, D. Barr, R. Snaith, W. Clegg, R. E. Mulvey, K. Wade and D. Reed, *J. Chem. Soc., Dalton Trans.*, 1987, 1071–1081.
17 A. L. Spek, *Acta Crystallogr.*, 2015, **C71**, 9–18.
18 C. F. Macrae, I. Sovago, S. J. Cottrell, P. T. A. Galek, P. McCabe, E. Pidcock, M. Platings, G. P. Shields, J. S. Stevens, M. Towler and P. A. Wood, *J. Appl. Crystallogr.*, 2020, **53**, 226–235.

